Rheol Acta (2010) 49:213–219
DOI 10.1007/s00397-009-0408-2

RAPID COMMUNICATION

On secondary loops in LAOS via self-intersection of Lissajous–Bowditch curves

Randy H. Ewoldt · Gareth H. McKinley

Received: 31 August 2009 / Accepted: 18 November 2009 / Published online: 12 December 2009

Abstract When the shear stress measured in large amplitude oscillatory shear (LAOS) deformation is represented as a 2-D Lissajous–Bowditch curve, the corresponding trajectory can appear to self-intersect and form secondary loops. This self-intersection is a general consequence of a strongly nonlinear material response to the imposed oscillatory forcing and can be observed for various material systems and constitutive models. We derive the mathematical criteria for the formation of secondary loops, quantify the location of the apparent intersection, and furthermore suggest a qualitative physical understanding for the associated nonlinear material behavior. We show that when secondary loops appear in the viscous projection of the stress response (the 2-D plot of stress vs. strain rate), they are best interpreted by understanding the corresponding elastic response (the 2-D projection of stress vs. strain). The analysis shows clearly that sufficiently strong *elastic* nonlinearity is required to observe secondary loops on the conjugate *viscous* projection. Such a strong elastic nonlinearity physically corresponds to a nonlinear viscoelastic shear stress overshoot in which existing stress is unloaded more quickly than new deformation is accumulated. This general understanding of secondary loops in LAOS flows can be applied to various molecular configurations and microstructures such as polymer solutions, polymer melts, soft glassy materials, and other structured fluids.

R. H. Ewoldt · G. H. McKinley (✉)
Hatsopoulos Microfluids Laboratory,
Department of Mechanical Engineering,
Massachusetts Institute of Technology,
Cambridge, MA, USA
e-mail: gareth@mit.edu

Keywords Nonlinear viscoelasticity · Large amplitude oscillatory shear (LAOS) · Lissajous–Bowditch curve · Stress overshoot

Introduction

Large amplitude oscillatory shear (LAOS) is a class of flow that is commonly used to characterize nonlinear viscoelastic material responses (Giacomin and Dealy 1993). In strain-controlled LAOS deformation, the imposed strain takes the form $\gamma(t) = \gamma_0 \sin \omega t$, which consequently subjects the sample to a corresponding oscillatory strain rate, $\dot{\gamma} = \gamma_0 \omega \cos \omega t$. The steady-state material stress response oscillates with the same fundamental period as the imposed deformation, $T = 2\pi/\omega$, but with a viscoelastic phase shift, as well as higher harmonic contributions when the imposed strain is high enough to induce material nonlinearity (Wilhelm 2002).

LAOS responses can be visualized as parametric curves (properly termed Lissajous–Bowditch curves) of the oscillating stress $\sigma(t)$ vs. strain $\gamma(t)$ or, alternately, stress $\sigma(t)$ vs. strain rate $\dot{\gamma}(t)$. More generally, this response can be represented in terms of closed space curves within a 3-D coordinate system with strain $\gamma(t)$, strain rate $\dot{\gamma}(t)$, and stress $\sigma(t)$ as the orthogonal coordinate axes (Fig. 1a). The 2-D Lissajous–Bowditch curves commonly represented in papers are then readily understood as projections of the fully 3-D coordinate space that describes the material response to oscillatory shearing. The 2-D projection onto the stress $\sigma(t)$ vs. strain $\gamma(t)$ plane views the material response from an elastic perspective (Fig. 1b), and a purely elastic mater-

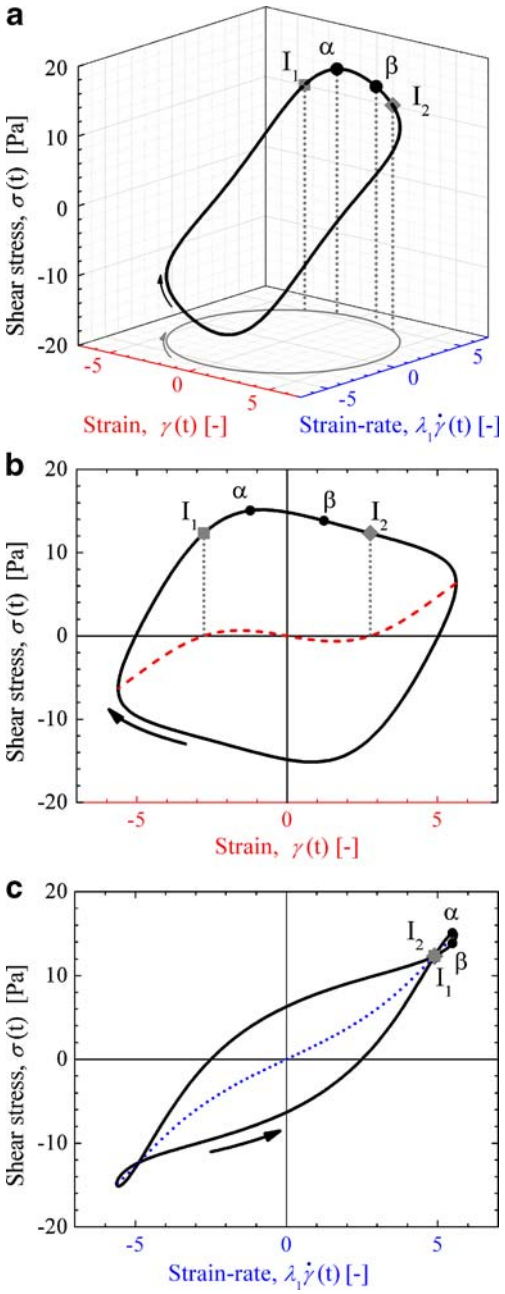

Fig. 1 LAOS simulation of the single-mode Giesekus model, Eq. 1, ($\lambda_1\omega = 1$, $\gamma_0 = 5.62$). Only the time-periodic steady-state response is shown, with *arrows* indicating the path trajectory. **a** 3-D Lissajous–Bowditch curve showing the stress response as a function of the orthogonal inputs, $\sigma(\gamma(t), \dot{\gamma}(t))$, **b** 2-D projection onto the plane of stress $\sigma(t)$ and strain $\gamma(t)$, including the instantaneous elastic stress $\sigma'(\gamma(t))$ (*dashed line*), and **c** 2-D projection onto the plane of stress $\sigma(t)$ and strain rate $\dot{\gamma}(t)$, including the instantaneous viscous stress $\sigma''(\dot{\gamma}(t))$ (*dotted line*). The viscous Lissajous–Bowditch curve in (**c**) shows apparent self-intersection at points I_1 and I_2, although the full-space curve represented in (**a**) does not intersect at these points

ial response would be a single-valued function of strain on this plane, $\sigma(\gamma)$. The viscous perspective is achieved by projecting the 3-D material trajectory onto the plane of stress $\sigma(t)$ vs. strain rate $\dot{\gamma}(t)$ as shown in Fig. 1c. In this work, we focus on the long-time steady-state oscillatory material response that is represented by a closed space curve; however, time-varying material responses associated with thixotropy, shear-induced migration, rheological aging, etc. can also be represented in this material-phase space by trajectories that slowly decay towards the corresponding periodic attractor.

We are interested here in the self-intersection of Lissajous–Bowditch curves which form "secondary loops" (Fig. 1c, points I_1 and I_2), a visually prominent phenomenon that quickly draws questions from the rheological observer. The interpretation of secondary loops has, to date, been limited to the study of specific material examples, being related to physical microstructural features such as non-affine deformation (Jeyaseelan and Giacomin 2008) and the absence of long-chain branching in polymer melts (Stadler et al. 2008). However, such secondary loops have been observed for many different material systems including micellar solutions (Ewoldt et al. 2008), a polystyrene solution (Jeyaseelan and Giacomin 2008), several molten polymers (Tee and Dealy 1975; Stadler et al. 2008), star-polymer networks (Rogers SA, Vlassopoulos D 2009, personal communication), as well as xanthan gum solutions and an invert-emulsion drilling fluid (Ewoldt et al. 2009). Nonlinear constitutive models can also show secondary loops; examples include a non-affine network model (Jeyaseelan and Giacomin 2008), a tube-based model of entangled linear polymers (Leygue et al. 2006; Stadler et al. 2008), and a single-mode Giesekus model (demonstrated here). Owing to the variety of systems which show secondary loops, we seek to provide a general interpretation of this nonlinear rheological phenomenon.

The mathematical criteria for the appearance of self-intersecting viscous Lissajous–Bowditch curves of stress $\sigma(t)$ vs. strain rate $\dot{\gamma}(t)$ have been considered previously by Stadler et al. (2008) and Burhin et al. (2008), who have identified multiple criteria which must be simultaneously satisfied by the higher harmonic components of the stress response. Here, we derive a single criterion which, for the most commonly observed case, is related to a *single* viscoelastic parameter $G'_M \equiv \frac{d\sigma}{d\gamma}|_{\gamma=0} < 0$. The parameter G'_M is the minimum strain elastic modulus as defined by Ewoldt et al. (2008). The criterion is understood through the connection between the 3-D Lissajous–Bowditch curves and the corresponding Chebyshev decomposition of the LAOS response. Furthermore, we address the theoretical possibility (unobserved to date) of self-intersection of the elastic projection of stress $\sigma(t)$ vs. strain $\gamma(t)$ and show, by analogy, that a single cri-

terion $\eta'_M < 0$ can be used to identify the conjugate phenomenon.

A general physical interpretation of the phenomenon is achieved, because the derived mathematical criteria are related to nonlinear viscoelastic material parameters. Our analysis suggests that a broad class of molecular and microstructural configurations can show this nonlinear rheological behavior; this short note, therefore, assists in the systematic interpretation of measured LAOS responses in terms of constitutive models and molecular structure.

Giesekus model example

A single-mode Giesekus model is used here as a canonical example in which secondary loops arise within a certain range of the Pipkin parameter space represented by frequency and strain amplitude (ω, γ_0). The constitutive equation for the Giesekus model, as presented by Bird et al. (1987), is given by

$$\begin{aligned} \sigma &= \sigma_s + \sigma_p \\ \sigma_s &= \eta_s \dot{\gamma} \\ \sigma_p + \lambda_1 \sigma_{p(1)} + \alpha \frac{\lambda_1}{\eta_p} \{\sigma_p \cdot \sigma_p\} &= \eta_p \dot{\gamma}. \end{aligned} \tag{1}$$

Here, σ_s is the solvent stress tensor, σ_p is the polymer stress tensor, $\sigma_{p(1)}$ is the upper convected time derivative of the polymer stress, η_s is the solvent viscosity, η_p is the polymer viscosity, λ_1 is the relaxation time, and α is the mobility factor which gives rise to a nonlinear viscoelastic response (for $\alpha \neq 0$). The LAOS simulation is performed as described by Ewoldt et al. (2008) using the following model parameters, $\lambda = 1$ s, $\eta_s = 0.01$ Pa s, $\eta_p = 10$ Pa s, and $\alpha = 0.3$. These four independent parameters result in a retardation time scale $\lambda_2 = \lambda_1 \eta_s / (\eta_s + \eta_p) = 0.001$ s and a polymeric shear modulus $G = \eta_p / \lambda_1 = 10$Pa. A wide range of frequencies and strain amplitudes were simulated (Ewoldt et al. 2008), $0.001 \leq \gamma_0 \leq 100$. Within this range, secondary loops were observed for a range of frequencies, $\lambda_1 \omega = 0.01 - 100$, at sufficiently large strain amplitude γ_0. Figure 1 shows the steady-state Lissajous–Bowditch curves associated with $\lambda_1 \omega = 1$, $\gamma_0 = 5.62$, for the single-mode Giesekus model, Eq. 1. Arrows are used to indicate the trajectory for each curve. Note that in the absence of secondary loops, elastic curves are traversed in a clockwise direction (Fig. 1b) whereas the corresponding viscous curves propagate counterclockwise (Fig. 1c). The viscous projection onto the 2-D plane of stress $\sigma(t)$ and strain rate $\dot{\gamma}(t)$ appears to intersect at points I_1 and I_2.

Criteria and interpretation of self-intersection

It is impossible for a full 3-D Lissajous–Bowditch curve to intersect itself within one period, since the controlled input coordinates $(\gamma(t), \dot{\gamma}(t))$ are orthogonal and always occupy unique values throughout a single cycle, i.e., the 2-D projection onto the plane of $(\gamma(t), \dot{\gamma}(t))$ does not intersect. However, a 2-D projection onto the other coordinate planes of $(\sigma(t), \gamma(t))$ or $(\sigma(t)\dot{\gamma}(t))$ has the opportunity to self-intersect because the individual inputs of strain $\gamma(t)$ or strain rate $\dot{\gamma}(t)$ take repeated values within a single period $T = 2\pi/\omega$. A sufficiently nonlinear response may thus result in a 2-D response curve *projection* that intersects itself and forms secondary loops, such as those which appear in the curve of Fig. 1c.

To proceed with the evaluation of a suitable quantitative criterion for self-intersection, we must introduce a mathematical representation of LAOS response curves. For an oscillatory strain input, $\gamma(t) = \gamma_0 \sin \omega t$, the viscoelastic stress response at steady-state can be written as a time-domain Fourier series of odd harmonics (Giacomin and Dealy 1993),

$$\sigma(t; \omega, \gamma_0) = \gamma_0 \sum_{n:\text{odd}} \left\{ G'_n(\omega, \gamma_0) \sin n\omega t + G''_n(\omega, \gamma_0) \cos n\omega t \right\}. \tag{2}$$

For sufficiently small strain amplitude γ_0, a linear material response is observed such that only the fundamental harmonic appears, $n = 1$ with a temporal phase shift δ_1 given by $\tan \delta_1 = G''_1 / G'_1$. For larger deformation amplitudes, higher harmonics appear, and the response is nonlinear. We argue that it is more meaningful to mathematically represent the measured material stress as a function of the time-varying kinematic inputs, strain $\gamma(t)$ and strain rate $\dot{\gamma}(t)$, rather than time itself. This is consistent with the closed space curve shown in Fig. 1c, $\sigma(\gamma(t), \dot{\gamma}(t))$. The stress response can be decomposed into a superposition of instantaneous elastic and viscous components (Cho et al. 2005), which are single-valued functions of normalized strain $x(t) = \gamma(t)/\gamma_0$ and normalized strain rate $y(t) = \dot{\gamma}(t)/\dot{\gamma}_0$, respectively. We write the superposition as $\sigma(t) = \sigma'(x(t)) + \sigma''(y(t))$. The decomposition into the elastic stress $\sigma'(x(t))$ and viscous stress $\sigma''(y(t))$ can then be written as a series of Chebyshev polynomials of the first kind (Ewoldt et al. 2008),

$$\begin{aligned} \sigma'(x; \omega, \gamma_0) &= \gamma_0 \sum_{n:\text{odd}} e_n(\omega, \gamma_0) T_n(x) \\ \sigma''(y; \omega, \gamma_0) &= \dot{\gamma}_0 \sum_{n:\text{odd}} v_n(\omega, \gamma_0) T_n(y) \end{aligned} \tag{3}$$

in which the elastic and viscous coefficients, e_n (ω, γ_0) and v_n (ω, γ_0), have a physical interpretation and are directly related to the time-domain Fourier coefficients of Eq. 2 via the expressions $e_n = G'_n(-1)^{\frac{n-1}{2}}$ and $v_n = G''_n/\omega$ (n : odd).

The (apparent) intersection locations, I_1 and I_2 (Fig. 1), are defined by the criterion that the shear stress in the material takes repeated values at the same shear rate but at different values of strain, $\sigma(\dot{\gamma}, \gamma_1) = \sigma(\dot{\gamma}, \gamma_2)$. If we consider the decomposition of stress into purely strain-dependent and rate-dependent contributions, then it is clear that this equality requires the total stress to be independent of the instantaneous strain at I_1 and I_2; therefore, the elastic stress must be instantaneously zero at these points (Fig. 1b). Thus, self-intersections of stress $\sigma(t)$ vs. strain rate $\dot{\gamma}(t)$ occur when

$$\sigma'(x(t)) = 0, \quad x \neq 0 \tag{4a}$$

where $x(t) = \gamma(t)/\gamma_0$. By analogy, self-intersection of the curve of stress $\sigma(t)$ vs. strain $\gamma(t)$ would occur if the decomposed viscous stress is instantaneously zero,

$$\sigma''(y(t)) = 0, \quad y \neq 0 \tag{4b}$$

where $y(t) = \dot{\gamma}(t)/\dot{\gamma}_0$. The criteria expressed in Eq. 4a, b are sufficiently general that they apply for any number of self-intersection or overlap points, e.g., for extreme nonlinearity in which multiple self-intersections occur. The criterion for a *single* self-intersection point (which has mirror symmetry about the origin) on a viscous response curve can be readily visualized in Fig. 1b which shows that the elastic stress is instantaneously zero, $\sigma'(\gamma(t)) = 0$, at the apparent intersection points I_1 and I_2. Correspondingly, Fig. 1c shows that the total stress is equal to the instantaneous viscous stress at points I_1 and I_2, i.e. $\sigma(t) = \sigma''(\dot{\gamma}(t))$.

Any self-intersection of the *viscous* projection therefore occurs when the instantaneous value of the decomposed *elastic* stress passes through zero at a non-zero value of the scaled strain $x(t) = \gamma(t)/\gamma_0$. This intersection point can be located by expanding the elastic stress in terms of the Chebyshev polynomials of the first kind (Eq. 2), $\sigma''(x) = \gamma_0\{e_1 x + e_3(4x^3 - 3x) + ...\}$. For a single self-intersection point with mirror symmetry, the criteria that $\sigma'(x_I) = 0$ at points I_1 and I_2 results in the leading order non-zero solution that the intersection points I_1 and I_2 occur at

$$x_I = \mp\frac{1}{2}\sqrt{3 - \left(\frac{e_1}{e_3}\right)}$$
$$y_I = \cos\left[\sin^{-1}(x_I)\right]. \tag{5}$$

in which x_I is required to be real, $x_I \in \mathbb{R}$, and $|x_I| < 1$. These conditions for x_I are achieved for $e_3/e_1 > 1/3$ or $e_3/e_1 < -1$,[1] i.e., the self-intersection of *viscous* curves results from sufficiently strong *elastic* nonlinearity. The visually dominant feature of the material nonlinearity thus appears as secondary loops on the *viscous* Lissajous–Bowditch projection, but it is best interpreted physically as a consequence of a nonlinear *elastic* phenomenon.

The general criterion in Eq. 4a applies for any number of possible self-intersections. Equation 5, however, must be extended to capture multiple intersections, since it was derived from a truncated polynomial expansion (to $n = 3$). For example, an expansion up to $n = 5$ can represent two mirror-symmetric intersection points. In this case, x_I is the solution to a biquadratic equation (omitted for sake of brevity), still subject to the conditions that $x_I \in \mathbb{R}$ and $|x_I| < 1$. This imposes combined constraints on the magnitudes of both e_5/e_1 and e_3/e_1 to identify zero, one, or two mirror-symmetric self-intersections. If this is extended further to an infinite series representation (see Eq. 2) then the quantitative criteria for just a single intersection would include the infinite set of coefficients e_n. Fortunately, such complicated criteria can be simplified for the most commonly observed self-intersection of the type shown in Fig. 1, as we show in the following discussion.

Without requiring truncation or leading order estimates, we now identify a single material parameter which corresponds to the formation of a single self-intersection with mirror symmetry, with the assumption that the total stress is positive at maximum positive strain $\gamma(t) = \gamma_0$ (e.g., a material response of the generic form shown in Fig. 1). Rather than searching the decomposed stresses for zero crossings (roots), we consider the general criterion for self-intersection, Eq. 4a, $\sigma'(x) = 0$ for $x \neq 0$, combined with the fact that the elastic stress $\sigma'(x)$ has odd symmetry about $x = 0$ with a necessary zero crossing at $x = 0$ (so that when the imposed strain $\gamma = 0$ we have an instantaneous elastic stress $\sigma' = 0$). Loops form when $\sigma'(x) = 0$ at locations other than $x = 0$, i.e., when multiple zero crossings are present. At the point of incipient loop formation, three real zero crossings (repeated roots) appear due to the odd symmetry of the elastic stress (Fig. 3). For three distinct zero crossings, the slope of the elastic stress $\sigma'(x)$ must change sign from positive, to negative, and back

[1] $e_3/e_1 < -1$ corresponds to negative total stress at maximum positive strain $\gamma = \gamma_0$, i.e., the material does not resist deformation but rather pushes towards further deformation. We are unaware of any observation of this type of behavior.

to positive (corresponding to an inflection point at the critical conditions for incipient loop formation). Therefore self-intersection is equivalent to development of a region in the center of the elastic stress curve which has negative slope, and which must occur at $x = 0$ to retain odd symmetry. Therefore, a sufficient quantitative criterion for a single self-intersection of a viscous Lissajous curve is a negative slope in the decomposed elastic stress located at $x = \gamma(t)/\gamma_0 = 0$,

$$\left.\frac{d\sigma'}{dx}\right|_{x=0} < 0. \tag{6}$$

By analogy, it is possible for the elastic projection of stress $\sigma(t)$ vs. strain $\gamma(t)$ to form secondary loops when sufficient viscous nonlinearity is present. The criteria for self-intersection of elastic Lissajous projections is

$$\left.\frac{d\sigma''}{dy}\right|_{y=0} < 0. \tag{7}$$

From a geometric viewpoint, the tangent slopes of the stress at these locations (Eqs. 6 and 7) correspond to viscoelastic material parameters introduced by Ewoldt et al. (2008). The minimum-strain elastic modulus G'_M, and the minimum-rate dynamic viscosity η'_M, are given in terms of the Chebyshev coefficients by the expressions

$$G'_M \equiv \left.\frac{d\sigma}{d\gamma}\right|_{\gamma=0} = \left.\frac{d\sigma'}{d\gamma}\right|_{\gamma=0} = e_1 - 3e_3 + 5e_5 - 7e_7 + \cdots \tag{8a}$$

$$\eta'_M \equiv \left.\frac{d\sigma}{d\dot\gamma}\right|_{\dot\gamma=0} = \left.\frac{d\sigma''}{d\dot\gamma}\right|_{\dot\gamma=0} = v_1 - 3v_3 + 5v_5 - 7v_7 + \cdots \tag{8b}$$

where $G'_M \equiv G'$ and $\eta'_M \equiv \eta'$ for a linear viscoelastic response, but in LAOS generally represent the instantaneous elastic modulus and dynamic viscosity at the minimum strains and strain rates, respectively. Note that these specific graphical definitions in terms of the local slopes of the *decomposed* stresses are equivalent to the local slopes of the *total* stress, as shown in Eq. 8a, b. Thus, $G'_M < 0$ and $\eta'_M < 0$ are equivalent to Eqs. 6 and 7. We remark that in extremely nonlinear cases multiple zero crossings may occur; therefore, multiple self-intersection points may appear theoretically. In such a case, the criteria given in Eq. 4a, b are still satisfied but the local slope at the origin will alternate between negative and positive with each additional loop. The criteria that $G'_M < 0$ and $\eta'_M < 0$ apply to the most commonly encountered experimental situation in which a single intersection point with mirror symmetry exists, and the total stress is positive at the extrema of loading, $\gamma(t) = \gamma_0$ and $\dot\gamma(t) = \dot\gamma_0$.

The criterion $G'_M < 0$ can also be interpreted geometrically with reference to the 3-D material response shown in Fig. 1. Points α and β are labeled in Fig. 1 to identify points at small finite strains $\mp d\gamma$ immediately before and after the strain is instantaneously zero, respectively (see Fig. 1b). Since the strain and strain rate inputs are related, points α and β also occur just before and just after the maximum positive strain rate is achieved, $\dot\gamma(t) = +\dot\gamma_0$ (c.f. Fig. 1c). The geometrical criterion for apparent self-intersection of a 2-D viscous projection ($\sigma(t)$ vs. $\dot\gamma(t)$) is that the stress at point β, denoted σ_β, must be smaller than the stress σ_α at point α. This corresponds to the constraint that $\frac{d\sigma}{d\dot\gamma}|_{\gamma=0} \equiv G'_M < 0$ (Fig. 1b).

In terms of the higher harmonic coefficients, in order to meet the criterion $G'_M = e_1 - 3e_3 + 5e_5 - \ldots < 0$, the third-harmonic elastic Chebyshev coefficient, e_3, must be sufficiently large and positive to induce apparent self-intersection of the viscous Lissajous–Bowditch curves,

$$\frac{e_3}{e_1} > \frac{1}{3}\left(1 + 5\frac{e_5}{e_1} - \cdots\right). \tag{9}$$

For completeness, we note that the corresponding criterion derived from Eq. 7 for self-intersection of the elastic curves would be

$$\frac{v_3}{v_1} > \frac{1}{3}\left(1 + 5\frac{v_5}{e_1} - \cdots\right). \tag{10}$$

Figure 2 shows the normalized Chebyshev spectrums for the Giesekus simulation of Fig. 1. Dashed lines are shown at $e_3/e_1 = 1/3$ and $v_3/v_1 = 1/3$ which indicate the leading order expressions for secondary loops to appear in either the viscous or elastic projection, respectively (however, we re-emphasize that the criteria for single-loop formation given by $G'_M < 0$ and $\eta'_M < 0$ are quite general and not limited to leading-order expressions such as Eqs. 9 and 10). As shown in Fig. 2, the third-harmonic elastic Chebyshev coefficient is sufficiently large and positive (i.e., $e_3/e_1 > 1/3$), that $G'_M < 0$ and secondary loops appear in the viscous Lissajous–Bowditch curves.

The fundamental physical interpretation is to recognize that a single self-intersection point appearing in the viscous projection of the material response corresponds to $G'_M < 0$. A negative slope indicates that the material is unloading elastic contributions to the instantaneous stress faster than new deformation is being accumulated (Ewoldt et al. 2008). If we consider the direction in which the space curve in Fig. 1 is traversed, then

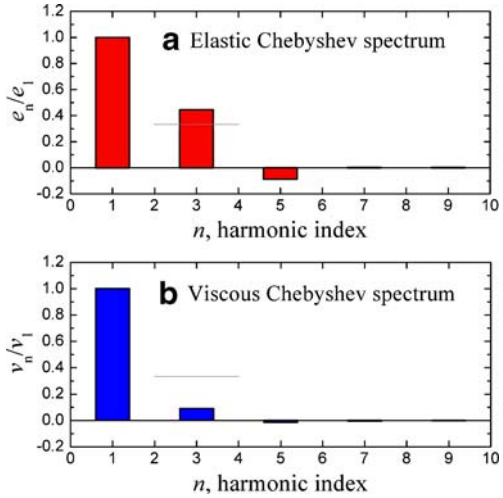

Fig. 2 Single-mode Giesekus model simulation, $\lambda_1\omega = 1$, $\gamma_0 = 5.62$; **a** the elastic Chebyshev spectrum shows that e_3/e_1 is sufficiently large and positive to create the secondary loops which appear in the viscous Lissajous–Bowditch curve (Fig. 1c). **b** The viscous Chebyshev spectrum. The *horizontal dashed lines* show the leading-order dimensionless criteria developed in Eqs. 9 and 10 for appearance of secondary loops

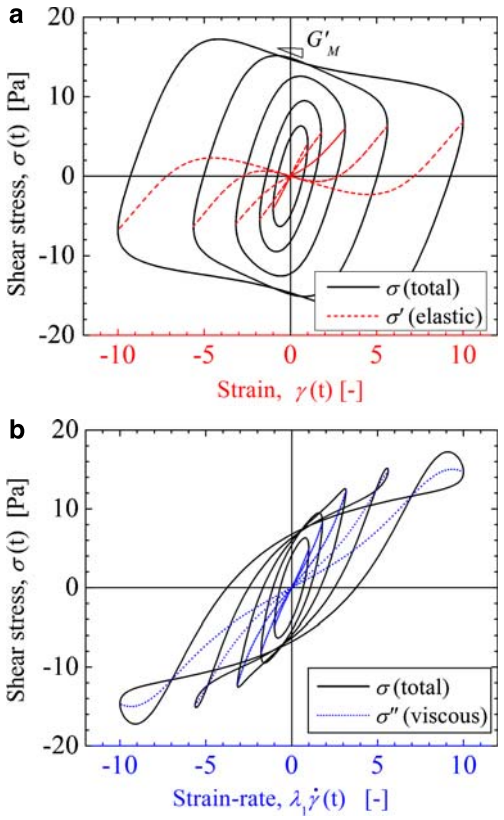

Fig. 3 Incipient secondary loop formation for the single-mode Giesekus model LAOS simulation, $\lambda_1\omega = 1$. **a** The elastic Lissajous–Bowditch projection, in which the criterion $G'_M < 0$ developed in the text corresponds to the appearance of repeated roots in the nonlinear elastic stress (*red curve*) and self-intersection and secondary loop formation in (**b**), the conjugate Lissajous–Bowditch projection of stress vs. shear rate

it is clear that from $\gamma = -\gamma_0$ to $\gamma = 0$ the strain rate $\dot{\gamma}(t)$ monotonically increases from zero to its maximum value. Self-intersection corresponds to the existence of a local maximum in stress (e.g., Fig. 1b) within this quadrant of the deformation cycle and is, therefore, interpreted as a viscoelastic stress overshoot. This overshoot is similar to the overshoot in the shear stress that may occur during startup of steady shear flow. Many nonlinear systems can show stress overshoot in the startup of steady shear. For example, the shear-enhanced disentanglement of polymer melts and solutions or the rupture of physical network structures can show strong stress overshoots. This overshoot behavior is characteristic of significant microstructural change which requires sufficiently large rates of deformation in concert with sufficient amplitude of deformation (Bird et al. 1987).

The Giesekus model exhibits stress overshoots during the inception of steady shear flow (Bird et al. 1987), and also in LAOS as indicated by $G'_M < 0$ and the appearance of secondary loops (Fig. 1, 3). In LAOS, we observe that a critical strain amplitude is required, e.g., for $\lambda_1\omega = 1$, secondary loops are not observed for $\gamma_0 \leq 3.16$, but at $\gamma_0 = 5.62$ we observe $G'_M < 0$ and secondary loops (Fig. 3). Additionally, we observe that a critical shear-rate is required. For lower frequencies, progressively larger strain amplitudes are needed such that $\lambda_1\omega\gamma_0 \gtrsim 10$ (for instance at $\lambda_1\omega = 0.01$ the range of strain amplitude was extended to $\gamma_0 = 1000$ in order to observe $G'_M < 0$ and the formation of secondary loops). The combined criteria of large strain amplitude *and* large strain rate amplitude are consistent with the typical criteria for stress overshoot in startup of steady shear (Bird et al. 1987). From the arguments and observations above, we conclude that stress overshoot is responsible for the appearance of secondary loops in viscous response curves with controlled-deformation oscillations.

An important distinction between LAOS and startup of steady shear is the periodic reversal of the flow field in LAOS. As we have noted, the oscillatory responses shown here are the steady periodic waveforms, thus any stress overshoot (i.e., a local maximum in elastic stress $\sigma'(x)$ which does not occur at $x = \pm 1$) must be reversibly achieved. Microstructures which breakdown irreversibly and cannot reform on the time scale of oscillation would not be expected to show stress overshoot and the corresponding secondary loops in steady-state LAOS deformations (although related features

may be observed in the initial transient response). For example, some polypropylene/organoclay nanocomposites show stress overshoot in reverse startup experiments only for sufficient rest times before reversal (Letwimolnun et al. 2007). Stress overshoots in LAOS would only be expected if the thixotropic restructuring timescale is smaller than the oscillatory deformation timescale. When this is the case, stress overshoot in steady-state LAOS tests may be anticipated, and LAOS may serve as a probe of thixotropic restructuring timescales. For example, disentangled polymer chains may have sufficient time to re-entangle, or soft glassy systems may find time to restructure during flow reversal and display reversible stress overshoot behavior.

Our analysis can be extended to controlled loading oscillations, e.g. $\sigma(t) = \sigma_0 \cos \omega t$, with appropriate decomposition of the resulting oscillatory strain response. It has recently been reported (Laeuger et al. 2009) that 4 wt.% aqueous xanthan gum solutions show loops in the stress response to strain-controlled inputs; however, such loops are absent in the strain response to stress-controlled inputs. This can be rationalized by our results here, since stress overshoots are a response to deformation inputs (just as in startup of steady shear), whereas strain overshoots typically do not arise in response to a stress input (e.g., creep loading at constant stress) unless the inertial effects are significant.

To summarize, we have shown that the apparent self-intersection of 2-D Lissajous–Bowditch curves corresponds to sufficiently large values of the third-harmonic components (Eq. 9) and that a single self-intersection point with mirror symmetry corresponds to G'_M or $\eta'_M < 0$ (Eqs. 6 and 7). More generally, any number of self-intersections can occur when the decomposed elastic or viscous stresses cross zero away from the origin, e.g., $\sigma'(x(t)) = 0$, $x \neq 0$, Eq. 4b. We find that self-intersection of 2-D Lissajous–Bowditch curve projections is most readily interpreted in terms of the complementary curve, i.e., the self-intersection of viscous projections is caused by a strong elastic nonlinearity. In this conjugate representation, the loops correspond to viscoelastic overshoot in the shear stress in the material and are analogous to the stress overshoot which occurs during the startup of steady shear flow. The distinction for LAOS is that the structural change associated with the overshoot must be at least partially reversible on the timescale of the oscillatory deformation and reoccur periodically. The signature of secondary loops may therefore act as a means of distinguishing various molecular and microstructural systems which show reversible stress overshoot behavior from those that exhibit nonlinearities originating from aging and thixotropy. This interpretation helps explain why secondary loops have been correlated with (and used to indicate) a lack of long-chain branching in polymer melts (Stadler et al. 2008), since branching may strongly modify stress overshoot behavior in an entangled material.

Finally, we note that apparent self-intersections and the appearance of secondary loops in the elastic Lissajous–Bowditch projections (i.e., plots of stress vs. strain) would correspond to pronounced overshoots in the instantaneous dissipative nature of a material (see Eq. 8b); for example a non-monotonic shear-thickening response. We are unaware of any experimental observations of such phenomena to date but they do not appear to be prohibited in principle.

References

Bird R, Armstrong R, Hassager O (1987) Dynamics of polymeric liquids: volume 1 fluid mechanics. New York: Wiley

Burhin HG, Bailly C, Keunings R, Rossion N, Leygue A, Pawlowski H (2008) A study of polymer architecture with FT-rheology and large amplitude oscillatory shear (LAOS). In: XV international congress on Rheology: The Society of Rheology 80th annual meeting, Monterey (California), The Society of Rheology, abstract booklet, EM18

Cho KS, Ahn KH, Lee SJ (2005) A geometrical interpretation of large amplitude oscillatory shear response. J Rheol 49(3):747–758

Ewoldt RH, Hosoi AE, McKinley GH (2008) New measures for characterizing nonlinear viscoelasticity in large amplitude oscillatory shear. J Rheol 52(8):1427–1458

Ewoldt RH, Winter P, Maxey J, McKinley GH (2009) Large amplitude oscillatory shear of pseudoplastic and elastoviscoplastic materials. Rheol Acta. doi:10.1007/s00397-009-0403-7

Giacomin AJ, Dealy JM (1993) Large-amplitude oscillatory shear. In: Collyer AA (ed.) Techniques in rheological measurement, Ch 4. London: Elsevier

Jeyaseelan RS, Giacomin AJ (2008) Network theory for polymer solutions in large amplitude oscillatory shear. J Non-Newton Fluid Mech 148(1–3):24–32

Laeuger J, Heyer P, Stettin H (2009) Different experimental methods to characterize the non-linear behavior of gels. In: The Society of Rheology 81st annual meeting, Madison, WI, Paper VS5

Letwimolnun W, Vergnes B, Ausias G, Carreau PJ (2007) Stress overshoots of organoclay nanocomposites in transient shear flow. J Non-Newton Fluid Mech 141(2–3):167–179

Leygue A, Bailly C, Keunings R (2006) A tube-based constitutive equation for polydisperse entangled linear polymers. J Non-Newton Fluid Mech 136(1):1–16

Stadler FJ, Leygue A, Burhin H, Bailly C (2008) The potential of large amplitude oscillatory shear to gain an insight into the long-chain branching structure of polymers. In: The 235th ACS national meeting, polymer preprints ACS, vol 49. New Orleans, LA, USA, pp 121–122

Tee TT, Dealy JM (1975) Nonlinear viscoelasticity of polymer melts. Trans Soc Rheol 19(4):595–615

Wilhelm M (2002) Fourier-Transform rheology. Macromol Mater Eng 287(2):83–105